

²C. A. Kapetanacos, D. A. Hammer, C. D. Striffler, and R. C. Davidson, *Phys. Rev. Lett.* **26**, 1303 (1973).

³O. Buneman, R. H. Levy, and L. M. Linson, *J. Appl. Phys.* **37**, 3203 (1966).

⁴R. H. Levy, *Phys. Fluids* **8**, 1268 (1965).

⁵W. Knauer, *J. Appl. Phys.* **37**, 602 (1966).

⁶C. K. Birdsall and J. R. Whimery, *J. Appl. Phys.* **24**, 314 (1953); C. K. Birdsall, G. R. Brewer, and A. V. Haeff, *Proc. I.R.E.* **41**, 865 (1953).

⁷R. J. Briggs, J. D. Daugherty, and R. H. Levy, *Phys. Fluids* **13**, 421 (1970).

⁸J. H. Malmberg and J. S. deGrassie, *Phys. Rev. Lett.* **35**, 577 (1975).

⁹J. S. deGrassie and J. H. Malmberg, *Phys. Fluids* **23**, 63 (1980).

¹⁰J. H. Malmberg and C. F. Driscoll, *Phys. Rev. Lett.* **44**, 654 (1980).

¹¹R. H. Levy, *Phys. Fluids* **11**, 920 (1968).

Fully Ionized and Total Silicon Abundances in the Alcator-C Tokamak

R. Petrasso, F. H. Seguin, and N. G. Loter

American Science and Engineering, Inc., Cambridge, Massachusetts 02139

and

E. Marmor and J. Rice

Massachusetts Institute of Technology, Cambridge, Massachusetts 02139

(Received 17 September 1982)

With use of x-ray imaging arrays, spatially and temporally resolved measurements were made of fully ionized and total absolute Si ($Z = 14$) densities following injection of Si into Alcator C. The fully stripped ions were detected through x rays resulting from ground-state radiative recombination. Central ion densities were found to be close to coronal equilibrium values. In addition, radial profiles of fully ionized and H-like Si showed large fluctuations during internal disruptions.

PACS numbers: 52.25.Fi, 32.30.Rj, 52.25.Gj, 52.70.-m

Impurity transport in tokamak plasmas is an important process, since it greatly affects plasma properties such as radiative losses.^{1,2} To study this transport, workers have purposely injected nonperturbing, trace amounts of moderate- Z (~ 14) impurities into plasmas.³⁻⁵ Until now such studies have been based on observed radiative emissions from partially stripped impurities, usually integrated along a single chord through the plasma cross section.³⁻⁵ Here we report the first spatially and temporally resolved measurements of fully ionized and total Si ($Z = 14$) abundances, which we made following injection of trace Si into Alcator C. Measurements were also obtained of fluctuations of impurity ion densities due to internal disruptions, a topic addressed only recently.⁶⁻⁸ The method we have used is based in part on detection of continuum x rays, principally from ground-state recombination of the fully stripped ion. (In a different context, fully stripped low- Z impurities, abundant within and intrinsic to the plasma, have been previously measured through charge exchange between fully stripped species and neutral particles.^{9,10}

Very recently this method has been applied, with use of a diagnostic neutral beam, to obtain spatially resolved measurements of C^{+6} and O^{+8} , if one assumes plasma discharge repeatability.¹⁰)

Si was injected, via the laser-blowoff method,³⁻⁵ into Alcator-C plasmas with central temperatures of 1.2 to 1.5 keV. Si transport was monitored by uv and x-ray spectrometers, and by two broadband, absolutely calibrated x-ray diode arrays¹¹ sensitive mainly to plasma radiation from inside a 10-cm radius (limiter radius is 16.5 cm). These arrays, the principal tools of this analysis, were usually filtered differently: The 17-detector "soft"-filtered array ($E \geq 1$ keV), filtered by 10.0 mg/cm² Be, responds mainly $K\alpha$ lines from H- and He-like Si (2.00 and 1.86 keV, respectively); the 10-detector "hard"-filtered array ($E \geq 3$ keV), filtered by 10.0 mg/cm² Be and 32.7 mg/cm² C, responds only to continuum x rays, primarily from ground-state radiative recombination of fully stripped and H-like Si. Even with allowance for the possibility of strong deviations from coronal equilibrium¹² (Fig. 1), fully stripped, H- and He-like ions

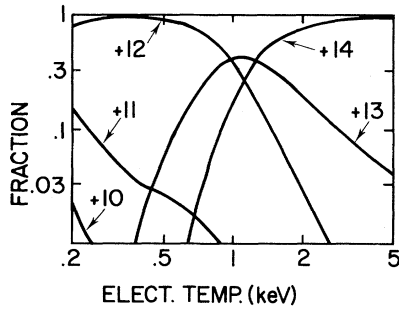


FIG. 1. Coronal equilibrium calculations of Si ion abundances (Ref. 12).

comprise essentially all of the Si inside a radius of 10 cm.

Calculations of the response of the arrays to the different charge states of Si included contributions from allowed transitions to ground states plus the $n=2$ forbidden and intercombination lines of Si XIII (Refs. 13 and 14) and bremsstrahlung and radiative recombination, with free-free and free-bound Gaunt factors included.^{15,16} The hard-filtered response to the most significant sources of continuum radiation is shown in Fig. 2; for $T_e \gtrsim 1.2$ keV (see also Fig. 1), the dominant term is ground-state radiative recombination of fully stripped ions, a term which has weak temperature dependence ($\sim T^{1/3}$) and which has been accurately calculated¹⁵ ($\approx 1\%$ error).

Each x-ray detector array provides (through Abel inversion) a time history of the radial profile of local plasma emissivity in a well-defined spectral passband. In each passband, the radiation of the injected Si may be isolated by subtracting the preinjection emissivity from the total emissivity at any post-injection time (as long as the injection occurs during the plateau stage), since it has been shown^{4,5} that the injected impurities do not affect the macroscopic characteristics of the background plasma and its radiation; for example, the emissions of the most important intrinsic impurities—C, N, O, and Mo (the limiter material)—as well as the electron cyclotron emissions were unchanged by the injections.

The observed local Si emissivities corresponding to soft and hard filtering (ϵ_A and ϵ_C , respectively) may be expressed as functions of the densities of the ionization states (N_{+i}):

$$\epsilon_A/n_e = A_{14}N_{+14} + A_{13}N_{+13} + A_{12}N_{+12},$$

$$\epsilon_C/n_e = C_{14}N_{+14} + C_{13}N_{+13} + C_{12}N_{+12},$$

where n_e is the measured electron density, and the A_i 's and C_i 's depend only on temperature

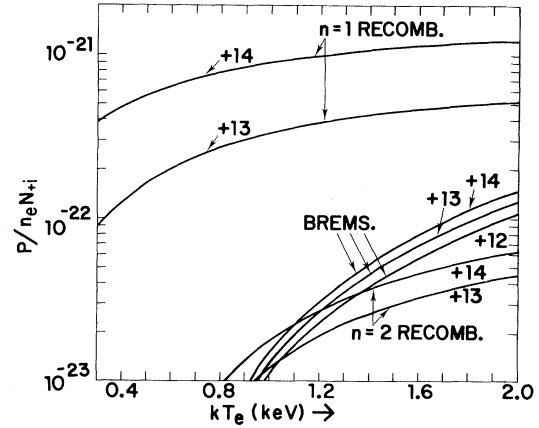


FIG. 2. Calculated system response, in units of $\text{erg cm}^3/\text{s}$, to various components of Si ion continuum radiation (normalized to $n_e N_{+i}$).

and filter response. (For example, C_{14} equals the sum of the “+14” terms shown in Fig. 2, plus the tiny contribution—of order 1%—of recombination terms with $n \geq 3$. At 1.5 keV, C_{14} is 2.3 and 16.0 times larger than C_{13} and C_{12} , respectively.) This gives us two equations with three unknowns, but by invoking one assumption—that coronal equilibrium exists between H- and He-like ions—we can solve for all three densities. This assumption can be justified *a posteriori* from our measurements, and it is also supported by our spectroscopic data. Of primary importance is the fact that the two quantities $N_{+14} + N_{+13} + N_{+12} = N_{\text{Si}}$ (the total Si density) are extremely insensitive to this assumption.

Figure 3 shows a sample x-ray diode output for a hydrogen discharge into which Si was injected. The x-ray flux rises as the Si penetrates

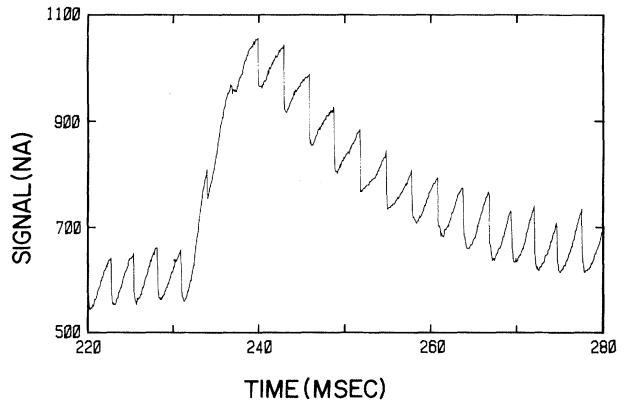


FIG. 3. Soft-filtered x-ray flux, integrated along a central chord of the plasma, around the time of a Si injection.

the plasma (at about 232 ms), and then decreases as the Si leaks out. For comparison to coronal predictions, we choose a time shortly after the Si emission has peaked, and average the data over a sawtooth cycle.

Figure 4 shows the results of this analysis for a deuterium discharge, illustrating the deduced density profiles and the profiles predicted on the basis of coronal equilibrium.¹² The predictions are normalized to the measured total Si profile (N_{Si}), after accounting for the effects of the electron temperature on the ionization state ratios (see Fig. 1). (The electron temperature profile was routinely determined from the electron cyclotron emissions.) At $r=0$ cm, the measured fully stripped abundance is 0.9 ± 0.4 times the coronal prediction. The uncertainty stems from errors in the absolute temperature measurement ($\pm 10\%$), and from the inverted x-ray data sets (the hard-filtered array had a partially obstructed field of view). We have not included the uncertainty associated with the coronal prediction, but the calculations unequivocally obtain their highest accuracy for the fully stripped state since, among other important reasons, the total recombination rate (for which no dielectronic component exists) has been calculated nearly exactly.¹⁷

From Fig. 4 we see that the coronal assumption for the H- to He-like ratio was thus justified; but even if this ratio were taken to be larger or smaller than coronal by a factor of 2, the derived values of N_{+14} and N_{Si} in the plasma core would change by no more than 15% and 2%, respectively. Thus, deviations of the fully ionized densities from coronal equilibrium are not large, at most a factor of ~ 2 . The proximity of our re-

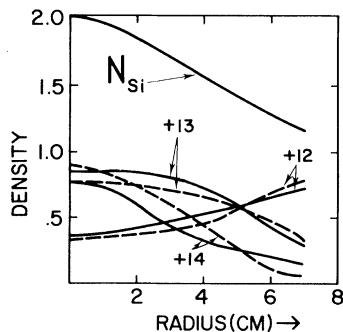


FIG. 4. Solid curves: Observed fully stripped (+14), H-like (+13), and He-like (+12) ion density profiles, and their sum (N_{Si}), in units of 10^{10} cm^{-3} . Dashed curves: Coronal predictions normalized to N_{Si} . The central electron density was $3.4 \times 10^{14} \text{ cm}^{-3}$.

sults to coronal equilibrium is mainly due to Alator's high electron densities ($3.4 \times 10^{14} \text{ cm}^{-3}$ for the discharge of Fig. 4); atomic relaxation times for ionization and recombination vary inversely with electron density, and for the highly ionized Si ions are ~ 2 ms. Coronal equilibrium pertains because this time is small compared to the shortest measured impurity confinement time for Si in hydrogen and deuterium discharges, ~ 10 and ~ 20 ms,⁵ respectively. In contrast, on PLT (Princeton Large Torus) the He- to Li-like ratio of intrinsic iron ions in the plasma core deviated by a factor of 7 from coronal predictions¹⁸; for their plasma conditions ($n_e \approx 2 \times 10^{13} \text{ cm}^{-3}$), radial transport times were comparable to or smaller than relevant ionization and recombination times. The general subject of coronal equilibrium, or the lack thereof, is important since radiative losses from a given impurity can be severely enhanced if its ionization states deviate significantly from coronal equilibrium.¹

Figure 5 shows the effects of an internal disruption on fully stripped ion densities, as derived from Si emissivity profiles just before and after an internal disruption. The post-disruption profile is seen to be strongly flattened in the plasma core, the central density decreasing by $\sim 50\%$. Regarding this result, several points should be noted. First, the changes in particle density are not a consequence of ionization or recombination, since the time scales for these processes (~ 2 ms) are much longer than the time scale of the disruption (~ 0.03 ms). Second, although disruption-induced changes in the electron temperature ($\sim 15\%$) and density ($\sim 4\%$) affect these calculations, their effects are small and the results are

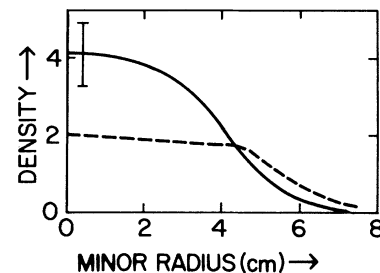


FIG. 5. Fully stripped Si ion density profiles, before (solid line) and after an internal disruption, in units of 10^{10} cm^{-3} . (The central electron density was $3.9 \times 10^{14} \text{ cm}^{-3}$.) The error bar shows the uncertainty in the difference between these two profiles; given the uncertainty, the profile change is consistent with conservation of the fully stripped particles.

insensitive to uncertainties in these quantities. (A reduction by a factor of 2 in the assumed temperature fluctuation results in a 10% change in the deduced N_{+14} fluctuation.) Finally, altering the H- to He-like ion ratio by a factor of 2 from coronal values changes the deduced N_{+14} fluctuation by only 6%. H-like profiles were also observed to be flattened by disruptions, with central values decreasing by $\sim 25\%$ (again relatively insensitive to the parameter variations described above). The percentage change is smaller than for the fully stripped species because the profile is less peaked (see Fig. 4), and flattening has a smaller effect. In either case the flattening presumably occurs through the same momentary enhancement of central radial transport which flattens electron temperature and density profiles,² as recently discussed.^{7,8}

In summary, a novel method has been used to measure—with spatial and temporal resolution—absolute abundances of fully stripped and total Si following the injection of trace Si into Alcator plasmas; with these and related measurements, certain important aspects of impurity transport were addressed. Because this measurement technique has the potential of extremely high accuracy, it should ultimately provide a very sensitive means for studying the transport of injected impurities in magnetically confined plasmas.

The authors thank the Alcator staff for their encouragement and assistance, especially R. Gandy for discussions about the electron cyclotron data. We express our gratitude to E. Källne and J. Källne of Smithsonian Astrophysical Observatory, and A. Krieger of American Science and Engineering, Inc. for helpful discussions. This work was supported by the U. S. Department of Energy under Contracts No. DE-AC02-77ET53068 and No. DE-AC02-78ET51013, and Massachusetts Institute of Technology under Contract No. MIT-FC-A-246206.

¹D. E. Roberts, Nucl. Fusion 21, 215 (1981), and references therein.

²R. Petrasso, M. Gerassimenko, F. H. Seguin, R. Krogstad, and E. Marmor, Nucl. Fusion 21, 881 (1981), and references therein.

³S. A. Cohen, J. L. Cecchi, and E. S. Marmor, Phys. Rev. Lett. 35, 1507 (1975).

⁴E. S. Marmor, J. E. Rice, and S. L. Allen, Phys. Rev. Lett. 45, 2025 (1980).

⁵E. S. Marmor, J. E. Rice, J. T. Terry, and F. H. Seguin, Massachusetts Institute of Technology Report No. PFC/JA-82-12, 1982 (to be published).

⁶E. Hinno *et al.*, Bull. Am. Phys. Soc. 25, 902 (1980).

⁷F. H. Seguin and R. Petrasso, in Proceedings of the Annual Sherwood Controlled Fusion Theory Conference, Santa Fe, New Mexico, 25–28 April 1982 (unpublished).

⁸F. H. Seguin, R. Petrasso, and E. S. Marmor, Massachusetts Institute of Technology Report No. PFC/JA-82-25, 1982 (to be published).

⁹R. C. Isler, L. E. Murray, S. Kasai, J. L. Dunlap, S. C. Bates, P. H. Edmonds, E. A. Lazarus, C. H. Ma, and M. Murakami, Phys. Rev. A 24, 2701 (1981).

¹⁰R. J. Fonck, M. Finkenthal, R. J. Goldston, D. L. Hendron, R. A. Hulse, R. Kaita, and D. D. Meyerhofer, Phys. Rev. Lett. 49, 737 (1982).

¹¹R. Petrasso, M. Gerassimenko, F. H. Seguin, J. Ting, R. Krogstad, P. Gauthier, W. Hamilton, A. T. Ramsey, P. Burstein, and R. Granetz, Rev. Sci. Instrum. 51, 585 (1980).

¹²J. M. Shull and M. Van Steenberg, Astrophys. J., Suppl. Ser. 48, 95 (1982), and 49, 351(E) (1982), and private communication.

¹³A. K. Pradhan, D. W. Norcross, and D. G. Hummer, Astrophys. J. 246, 1031 (1981).

¹⁴R. Mewe, J. Schrijver, and J. Sylwester, Astron. Astrophys. 87, 55 (1980), and references therein.

¹⁵W. J. Karzas and R. Latter, Astrophys. J., Suppl. Ser. 6, 167 (1961).

¹⁶R. T. Brown, Astrophys. J. 170, 387 (1971). (Typographical errors need to be corrected before applying Brown's formula.)

¹⁷M. J. Seaton, Mon. Not. Roy. Astron. Soc. 119 (2), 81 (1959).

¹⁸M. Bitter, S. von Goeler, P. S. Efthimion, M. Goldman, K. W. Hill, and N. Sauthoff, Bull. Am. Phys. Soc. 26, 981 (1981), and private communication.